AIAA JOURNAL
Vol. 31, No. 10, October 1993

Smooth Contact of Orthotropic Laminates by Rigid Cylinders

Enboa Wu,* Jey-Chung Chao,† and Ching-Shih Yen†
National Taiwan University, Taipei, 106 Taiwan, Republic of China

An analytical method is developed to investigate the contact behavior of an orthotropic laminate indented by a frictionless cylinder. The method is derived from an exact Green's function, which is based on the anisotropic elasticity theory in the plane strain condition. The contact response of a laminate is characterized into small and large contact stages depending on conformation of the curvatures between the indenter and the laminate in the contact region. The large contact stage occurs after conformation of the curvatures, resulting in less stress concentration in the laminate. It is found that the large contact stage readily develops when large indenters or large laminate span-to-thickness ratios are used. Also, the effect of slight misalignment of an indenter on the contact response of the laminate is significant. On the other hand, a change of laminate stacking sequence has an insignificant effect on the force-indentation relationship.

Introduction

In testing the flexural and shear strengths of a composite laminate, three- or four-point bending tests are standard in the industry. Up to now, the American Society for Testing and Materials (ASTM) D790 Standard, which adopts the strength of material approach, is still the most commonly used in the aerospace industry. The actual stresses and strains, however, have been found to deviate significantly from those predicted by this elementary approach. Many researchers have devoted efforts to understanding the contact phenomena because study of the stress distribution in a composite specimen during a flexural test is essentially equivalent to investigating a contact problem involving a composite beam and rigid cylindrical indenters. For example, Berg et al.[1] used finite element methods to analyze the shear stress distribution in a short orthotropic beam when an applied load is uniformly distributed over a small length of its upper surface. They found that the stresses deviate drastically from those predicted by the classical beam theory. The same phenomenon was observed later by other researchers using different methods.[2-4] It was also found that the contact pressure distribution is neither uniform nor in an elliptic profile of Hertz when a beam is deflected. To investigate this phenomenon, various analytical methods were developed to study the actual pressure distribution and the response of beams under indentation by smooth and rigid indenters. The approaches, which superimposed elasticity solutions on pure bending theory solutions of beams, were frequently employed to study the contact behavior of isotropic[5,6] or orthotropic[7,8] beams. Recently, Green's function approaches that simplify the formulation were used. For example, Sankar developed approximate Green's functions to solve for the contact problem by either a numerical procedure[9] or a closed-form solution.[10] This approach, however, requires solving for two approximate Green's functions and imposing constraints on indenters. The two Green's functions are obtained from half-plane and beam solutions. In addition, these efforts were all devoted to solving problems involving isotropic or orthotropic beams, and the focuses were mainly on the pressure profile and the load-deflection relationship of these homogeneous beams. The contact problem involving laminated beams was never addressed. Further, the stress distribution in a beam at different loading levels inside the specimen and the effect of slight loading eccentricity of an indenter were never studied. This loading eccentricity is frequently encountered in a flexural test. Similarly, the stresses inside a specimen are what cause the specimen to fail. Therefore, this paper aims to study the contact response of orthotropic *laminates*. Also, contact stresses and the effect of loading eccentricity will be investigated.

In this paper, an exact Green's function is constructed using the anisotropic elasticity theory in the plane strain condition. The Green's function applies to a laterally loaded orthotropic laminate of infinite width as long as the laminate is simply supported and the loading can be expanded by Fourier series. The indenter is assumed to be smooth, thus the effect of friction is not considered. The Green's function is derived from an exact solution developed previously by Pagano.[11] The force-indentation, force-contact length relationships and the pressure distribution of orthotropic laminates are first studied. The response of the laminates is characterized into small and large contact stages, where the stress concentration phenomenon in the contact region inside the laminate is very different. The effects of changing indenter size, span-to-thickness ratio, and stacking sequence of the laminates are then investigated. The significant effect due to small loading eccentricity of an indenter is also analyzed.

Solution Method

The laminate considered is an infinite strip in the y direction and is simply supported, as shown in Fig. 1. A rigid cylinder acts on the upper surface of the laminate in the central region but may not be at the center of the laminate. The plane strain condition is imposed in the following derivation. Therefore,

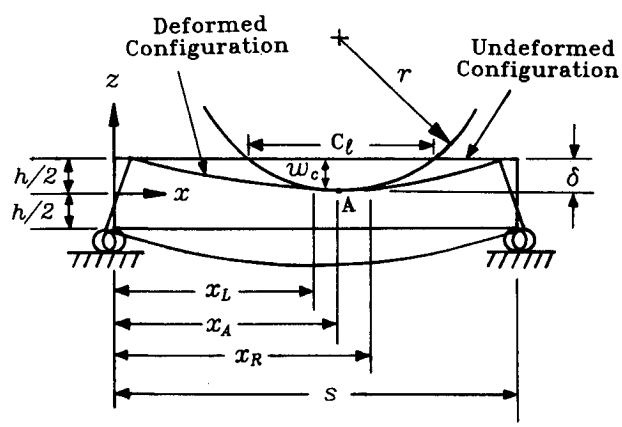

Fig. 1 Composite laminate indented by cylindrical indenter.

Received Aug. 1, 1992; revision received Feb. 17, 1993; accepted for publication Feb. 28, 1993.

*Associate Professor, Institute of Applied Mechanics.
†Graduate Student, Institute of Applied Mechanics.

the constitutive relationship for each layer of the laminate is expressed as

$$\epsilon_x^i = \bar{S}_{11}^i \sigma_x^i + \bar{S}_{13}^i \sigma_z^i$$
$$\epsilon_z^i = \bar{S}_{13}^i \sigma_x^i + \bar{S}_{33}^i \sigma_z^i \tag{1}$$
$$\gamma_{xz}^i = \bar{S}_{55}^i \tau_{xz}$$

where i represents the ith lamina and $\bar{S}_{ij}$ are the reduced compliance coefficients for plane strain. Throughout this paper, only orthotropic laminates are considered. Thus, in compliance with the contracted notation used in Eq. (1), the one, two, and three axes of each layer are always in the directions of the x, y, and z axes, respectively, regardless of lamina orientations (Fig. 1). The relationship between $\bar{S}_{ij}$ and the elasticity compliance S_{ij} is

$$\bar{S}_{11} = S_{11} - \frac{S_{12}^2}{S_{22}}; \qquad \bar{S}_{13} = S_{13} - \frac{S_{12}S_{23}}{S_{22}}$$
$$\bar{S}_{33} = S_{33} - \frac{S_{23}^2}{S_{22}}; \qquad \bar{S}_{55} = S_{55}$$

The boundary conditions on the two simple supports are defined as

$$\sigma_x^i(0, y) = \sigma_x^i(s, y) = 0$$
$$w^i(0, y) = w^i(s, y) = 0 \tag{2}$$

where s is the span of the laminate and w^i is the displacement in the z direction for the ith lamina. By using the infinitesimal strain theory, the solution to such an orthotropic laminate was obtained by Pagano under the following loading condition[11]:

$$\sigma_z\left(x, \frac{h}{2}\right) = c \sin px, \qquad p = \frac{n\pi}{s}$$
$$\sigma_z\left(x, \frac{-h}{2}\right) = \tau_{xz}\left(x, \pm\frac{h}{2}\right) = 0 \tag{3}$$

where c is a constant. The obtained transverse displacement of the ith layer for the loading condition given by Eq. (3) is

$$w_n^i(x, z) = \sin px \sum_{j=1}^{4} A_{ji}\left(\bar{S}_{13}^i m_{ji} - \frac{\bar{S}_{33}^i}{m_{ji}} p^2\right)\exp(m_{ji} z_i) \tag{4}$$

where A_{ji} can be solved using Eq. (3) and the interface continuity conditions, i.e.,

$$\sigma_z^i\left(x, -\frac{h_i}{2}\right) = \sigma_z^{i+1}\left(x, \frac{h_{i+1}}{2}\right)$$
$$\tau_{xz}^i\left(x, -\frac{h_i}{2}\right) = \tau_{xz}^{i+1}\left(x, \frac{h_{i+1}}{2}\right)$$
$$u^i\left(x, -\frac{h_i}{2}\right) = u^{i+1}\left(x, \frac{h_{i+1}}{2}\right) \tag{5}$$
$$w^i\left(x, -\frac{h_i}{2}\right) = w^{i+1}\left(x, \frac{h_{i+1}}{2}\right)$$

Note that

$$\left.\begin{matrix} m_{1i} \\ m_{2i} \end{matrix}\right\} = \pm p\left(\frac{\alpha_i + \beta_i}{\gamma_i}\right)^{1/2}; \qquad \left.\begin{matrix} m_{3i} \\ m_{4i} \end{matrix}\right\} = \pm p\left(\frac{\alpha_i - \beta_i}{\gamma_i}\right)^{1/2} \tag{6}$$

and

$$\alpha_i = 2\bar{S}_{13}^i + \bar{S}_{55}^i$$
$$\beta_i = (\alpha_i^2 - 4\bar{S}_{11}^i \bar{S}_{33}^i)^{1/2} \tag{7}$$
$$\gamma_i = 2\bar{S}_{11}^i$$

Let the contact load be expressed by

$$q(x) = \sum_{n=1}^{\infty} a_n \sin px \tag{8}$$

where

$$a_n = \frac{2}{s}\int_0^s q(x)\sin px \, dx \tag{9}$$

Thus, the lateral displacement $w(x, z)$ of a laminate caused by an indenter can be expressed using the superposition principle:

$$w(x, z) = \sum_{n=1}^{\infty} a_n w_n(x, z) \tag{10}$$

$$= \int_0^s \left[\frac{2}{s}\sum_{n=1}^{\infty} w_n(x, z)\sin\frac{n\pi}{s}\xi\right] q(\xi)\, d\xi \tag{11}$$

Furthermore, Eq. (11) can be expressed in the form of a Green's function:

$$w(x, z) = \int_0^s G(x, z; \xi) q(\xi)\, d\xi \tag{12}$$

where

$$G(x, z; \xi) = \frac{2}{s}\sum_{n=1}^{\infty} w_n(x, z)\sin\frac{n\pi}{s}\xi \tag{13}$$

The meaning of $G(x, z; \xi)$ is the displacement at (x, z) due to unit lateral load applied on the upper surface of the laminate at $(\xi, h/2)$.

Equation (12) can be expressed in the following form if a contact problem is considered:

$$w_c(x, h/2) = \int_{x_L}^{x_R} G(x, h/2; \xi) q(\xi)\, d\xi \tag{14}$$

where $x \in [x_L, x_R]$ is in the contact region (Fig. 1) and $q(\xi)$ is the pressure within the contact zone. Figure 1 also depicts the deformed and original configurations of the laminate.

If a rigid cylindrical indenter is used, $w_c(x, h/2)$ can be expressed as

$$w_c(x, h/2) = -\delta + [r - \sqrt{r^2 - (x - x_A)^2}] \tag{15}$$

where δ is the indenter movement, r is the radius of the cylinder, and x_A is the first contact point at the upper surface of the laminate. If there is no loading eccentricity, x_A is at the center of the upper surface of the laminate.

Because both the contact length $[x_L, x_R]$ and the pressure distribution $q(\xi)$ are unknown, the exact solution to Eq. (14) is not available. Thus, a numerical procedure is developed. The procedure starts with selecting a sufficiently large contact length that must include the actual contact length. A typically selected contact length is C_l, as shown in Fig. 1. The selected contact zone is divided into n subsets of equal length a. By assuming a constant pressure q_i inside each subset, the following equation is obtained:

$$w_c(x_j, h/2) = \sum_{i=1}^{k} q_i \int_{x_i - a/2}^{x_i + a/2} G(x_j, h/2; \xi)\, d\xi \tag{16}$$

where x_i is the center of the ith subset. Because w_c and all of the

$$\int_{x_i - a/2}^{x_i + a/2} G(x_j, h/2; \xi)\, d\xi \qquad i = 1, \ldots, n$$

are known from Eqs. (15) and (13), respectively, the pressure distribution q_i, $i = 1, \ldots, n$, can be calculated accordingly. However, an additional criterion for compressive contact pressure, i.e., $q_i \le 0$, must be satisfied to obtain a feasible solution. Therefore, the subsets that have positive pressure

values are removed and Eq. (16) is executed again. This procedure proceeds until all of the contact pressure values are in compression in the remaining subsets. This numerical procedure has been successfully employed to study the contact behavior of laminated plates indented by a rigid sphere.[12] Normally, in our calculation it takes less than five iterations to reach the final solution.

To calculate the contact pressure accurately, a refined discretization of the contact zone of a laminate is needed. Also, the number of Fourier sine terms has to be sufficiently large to suitably represent the constant pressure within each of the discrete subsets. As a consequence, a convergence test is needed to select both the numbers of discrete pressure subsets and Fourier terms. In this study, the check scheme is similar to that in Whitney.[4] For example, if the length of a selected subset for a unit pressure loading is $a = (1/1600)s$, where s is the span of a laminate, 500 Fourier sine terms only give approximately 30% of the original unit magnitude, and the pressure oscillates beyond the subset boundaries, as shown in Fig. 2a. However, if 2000 Fourier sine terms are used in Eq. (8), the unit pressure can be well approximated. Figure 2b depicts this simulation. In the following analyses, convergence is always checked for each run.

Results

In the subsequent analyses, T300/976 graphite/epoxy is used. The material properties for the unidirectional laminas are[13]: $E_L = 156$ GPa, $E_T = 9.09$ GPa, $G_{LT} = 6.96$ GPa,

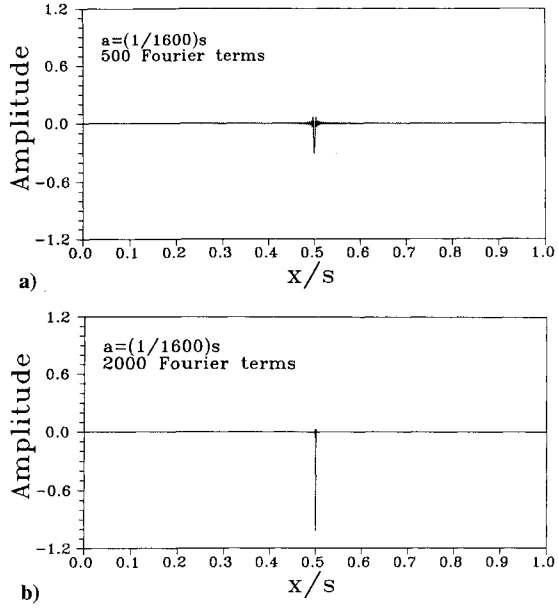

Fig. 2 Uniform pressure of unit magnitude constructed by a) 500 and b) 2000 Fourier sine terms laterally applied on center of laminate.

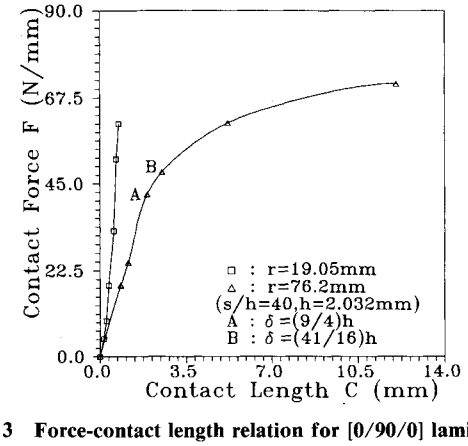

Fig. 3 Force-contact length relation for [0/90/0] laminate.

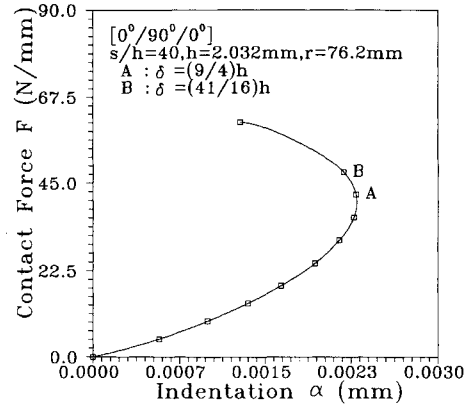

Fig. 4 Force-indentation relation for [0/90/0] laminate.

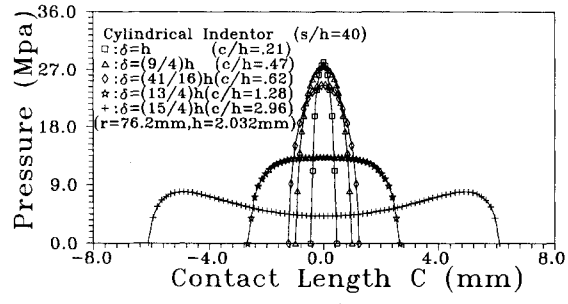

Fig. 5 Contact pressure distribution on [0/90/0] laminate.

$G_{TT} = 3.24$ GPa, $\nu_{LT} = 0.228$, and $\nu_{TT} = 0.400$, where L and T represent the directions parallel and perpendicular to the fibers, respectively, and E, G, and ν are the Young's modulus, shear modulus, and Poisson's ratio, respectively. To be consistent with the contracted notation and the plane strain condition used in Eq. (1), the subscript L corresponds to the first or second axis for a unidirectional lamina aligned in the x or y direction, respectively. Also, indentation α is defined as the difference between the indenter movement distance δ and the deflection of the distal side of the laminate.

Contact Phenomenon Characterization

In the following study, the rigid indenter used is 76.2 mm in radius. The span-to-thickness ratio of a 2.032-mm-thick [0/90/0] symmetric laminate is 40. This ratio is usually used in the flexural test for composite specimens. In Figs. 3-5, it is found that the laminate response can be characterized into small and large contact stages, and point A in Figs. 3 and 4 is to separate these two stages. Note that F represents force per unit width.

In the small contact stage, the force-contact length, F—C, relationship for the [0/90/0] laminate is approximately linear, as shown in Fig. 3. This phenomenon is similar to those predictions in isotropic[6] and orthotropic[8,9] beams. The curve for the 19.05-mm indenter will be discussed in the next subsection. The slope of the force-indentation, F—α, curve shown in Fig. 4 grows progressively and reaches an infinite value at point A, which is at the extremity in the small contact stage.

Beyond point A, the laminate is in the large contact stage. The contact length increases drastically when a small amount of additional force is added to the laminate, as shown in Figs. 3 and 5. With this small additional load, the indentation decreases and results in a "rebound" phenomenon in the force-indentation relationship, as shown in Fig. 4. Furthermore, it is found from Fig. 5 that the pressure peak drops significantly and the profile changes from an ellipse to a saddle shape.

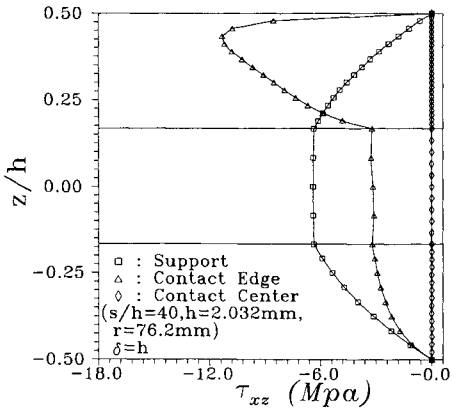

Fig. 6 Shear stress in [0/90/0] laminate at $\delta = h$.

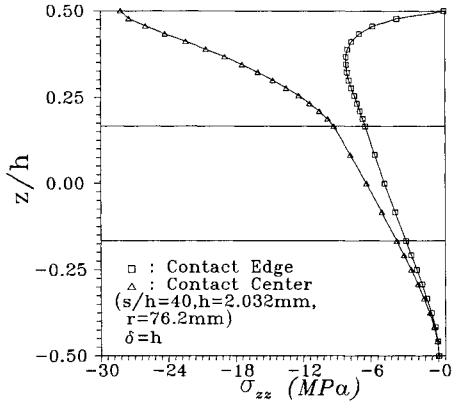

Fig. 7 Through-the-thickness normal stress in [0/90/0] laminate at $\delta = h$.

The occurrence of the different contact phenomena in these two stages can be explained by the "curvature conformation" between a centrally loaded laminate and a cylindrical indenter, as was similarly observed in isotropic[6] and orthotropic beams.[9] In the small contact stage, the radius of curvature of the cylinder ($r = 76.2$ mm) is much smaller than that of the [0/90/0] laminate near the contact region. Therefore, the contact area is smaller, the pressure loading is more concentrated, and the slope of the force-indentation curve is smaller. As the indenter movement gets larger, the laminate curvature gradually conforms to that of the indenter. It results in drastic increase of the contact area that, in turn, reduces the pressure peak and forces the slope of the F—α curve to change from positive to negative values.

The curvature conformation is also found to influence the laminate stress distribution significantly in the contact neighborhood. In the small contact stage, stress concentration occurs near and within the contact region in the laminate because of the curvature mismatch. Figures 6 and 7 show distribution of τ_{xz} and σ_{zz}, respectively, for $\delta = h$, which is in the small contact range. In Fig. 6, stress concentration is found to be near the upper surface of the [0/90/0] laminate at the contact edge, whereas the degree of this local shear stress concentration is much reduced in the large contact stage, as is depicted in Fig. 8. Figure 8 is for $\delta = (41/16)h$ and is in the early stage of large contact. The effect of curvature conformation between the indenter and the laminate is found to be more significant for σ_{zz}. In Fig. 9, the maximum value of σ_{zz} for $\delta = (41/16)h$ is even smaller than that in Fig. 7, which is for $\delta = h$. Decrease of the σ_{zz} values at the contact center when the laminate deflects more can also be observed from the pressure distribution plotted in Fig. 5. Thus, laminates may be crushed in the thickness direction at a smaller rather than at a larger contact load. On the other hand, stress concentration becomes much less significant as the indenter moves even deeper due to the curvature conformation.[14]

Unlike the distributions of τ_{xz} and σ_{zz}, the distribution shape of σ_{xx} is not much affected by indentation under the pressure loading plotted in Fig. 5. Figure 10 shows σ_{xx} at $\delta = h$, which is in the small contact stage. The effect of curvature mismatch in this small contact stage only produces slight stress concentration near the contact surface in the laminate. This stress concentration is further reduced as the laminate advances into the large contact stage.[14]

Effect of Indenter Size

A [0/90/0] laminate of $h = 2.032$ mm and a span-to-thickness ratio of $s/h = 40$ is used. To investigate the effect of the indenter size on the contact behavior, cylinders that are 9.525, 19.05, and 76.2 mm in radii are employed. In Fig. 11, it is found that the laminate indented by the largest indenter has

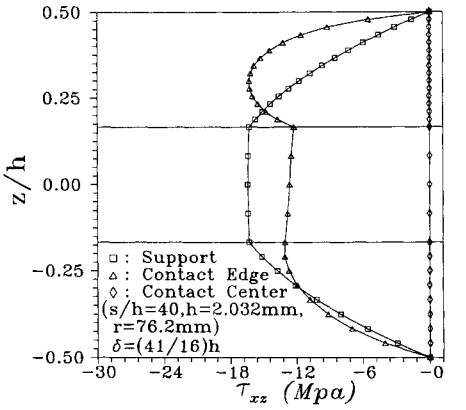

Fig. 8 Shear stress in [0/90/0] laminate at $\delta = (41/16)h$.

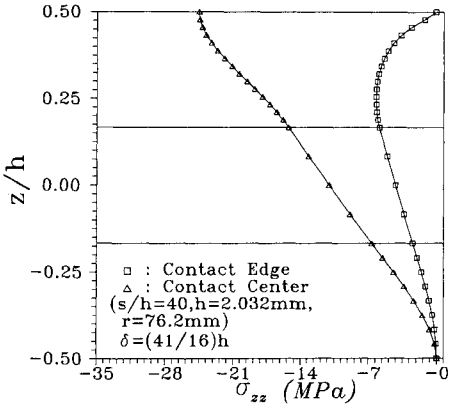

Fig. 9 Through-the-thickness normal stress in [0/90/0] laminate at $\delta = (41/16)h$.

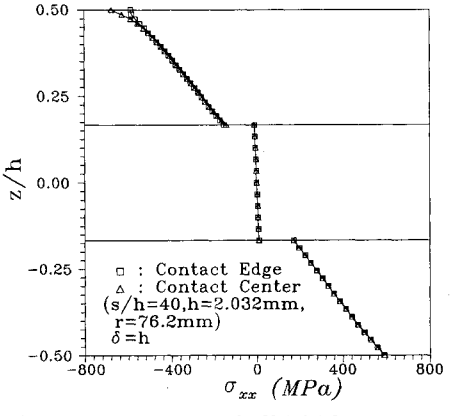

Fig. 10 In-plane normal stress in [0/90/0] laminate at $\delta = h$.

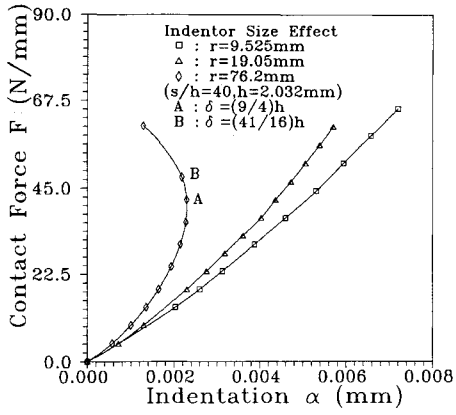

Fig. 11 Effect of indenter size on F—α relation for [0/90/0] laminate.

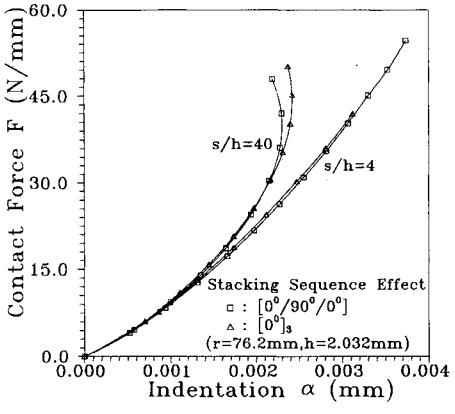

Fig. 12 Effect of laminate stacking sequence on F—α relation, $s/h = 4$ and 40.

conformed to the curvature of the indenter at the contact region. As a result of this conformation, the laminate advances into the large contact stage and the stress concentrations are much reduced in the contact neighborhood of the laminate. However, due to the inconsistency of the curvatures between the two smaller cylinders and the laminates, all of the three stress components have locally high stresses. These high stresses will cause early damage of composite specimens during flexural testing.

The effect of using different indenter sizes is also found by looking at the force-contact length relationship. In Fig. 3, a nearly straight line for the F—C relationship is obtained up to a force level of 60.75 N/mm for the 19.06-mm radius indenter. This nearly linear relationship also shows that the laminate is still in the small contact stage, and the laminate curvature in the contact neighborhood has not yet conformed to that of the indenter. But the contact length for the indenter of 76.2 mm in radius has increased drastically at this loading level, which indicates that the laminate is in the large contact stage.

Effect of Stacking Sequence

The stacking sequences considered are [0/90/0] and [0], both with a thickness of $h = 2.032$ mm. Because the span-to-thickness ratio also affects the contact behavior, the s/h ratios of 4 and 40 are used. The indenter used is 76.2 mm in radius. The results are shown in Fig. 12. It is found that using different stacking sequences results in essentially the same force-indentation relationship in the small contact stage for both cases. However, when the load gets larger, the laminate with $s/h = 40$ advances gradually into the large contact stage because the F—α curves start to rebound, whereas the laminate with $s/h = 4$ is always in the small contact stage within the current analysis range. Further, once the laminates start to advance into the large contact stage, the unidirectional specimen shows larger indentation for the same applied load due to the stronger flexural stiffness.

Effect of Span and Thickness

It has been shown in Fig. 12 that the F—α relationship is essentially the same in the small contact stage for laminates with s/h ratios of 4 and 40. However, the laminate with longer span advances to the large contact stage earlier, and stress concentration in the contact neighborhood is expected to be less significant. In Fig. 13, it is shown that the effect of changing laminate thickness on the F—α relationship is significant. Here, [0/90/0] laminates of $s = 81.28$ mm and indenters of 76.2 mm in radius are used. The slopes of force-indentation curves decrease and converge into approximately a straight line as the laminate thickness increases from $h = 2.032$ to 16.256 mm, i.e., $s/h = 40$ to 5. Apparently, the large contact

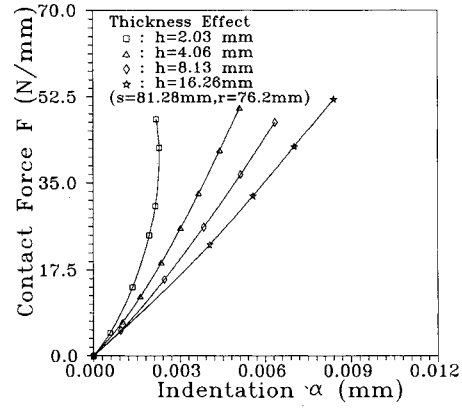

Fig. 13 Effect of laminate thickness on F—α relation for [0/90/0] laminate.

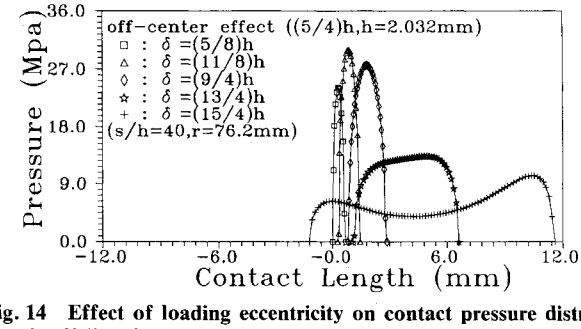

Fig. 14 Effect of loading eccentricity on contact pressure distribution for [0/90/0] laminate.

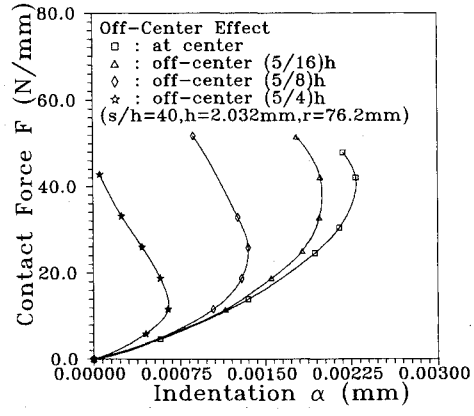

Fig. 15 Effect of loading eccentricity on F—α relation for [0/90/0] laminate.

stage does not exist for the thicker laminates within the analysis range. This is because an increase of the laminate thickness prevents the curvature conformation between the indenter and the laminate from prevailing until a much later time. Thus, a higher local stress concentration is expected to occur in thicker laminates under the same contact loading.

By comparing Fig. 12 with Fig. 13, it is found that change of the laminate thickness has a more significant effect on the $F-\alpha$ relationship. This is because the curves in Fig. 13 deviate at the beginning of the contact process.

Effect of Loading Eccentricity

In a flexural test using either composite or isotropic specimens, a small amount of loading eccentricity due to misalignment of the indenter may occur and may affect the local contact behavior of laminates. Three different eccentricities of $(5/16)h$, $(5/8)h$, and $(5/4)h$, corresponding to 0.635, 1.27, and 2.54 mm off-center distance, respectively, are investigated. The laminate thickness is $h = 2.032$ mm. The indenter is 76.2 mm in radius. The span-to-thickness ratio is 40; [0/90/0] lay-ups are used.

Figure 14 shows the pressure distribution in the case of an off-center distance of $5h/4 = 2.54$ mm to the right. The origin of the horizontal axis in the figure is at the center of the laminate. It is found that, as the contact force increases, the pressure distribution not only shifts progressively to one side, but the pressure distribution itself becomes asymmetric. As a result of this asymmetric pressure distribution, the stress distribution in the laminate is different from that under centric loading, and a different damage mechanism may occur. Therefore, it is important to align an indenter at the central position on a specimen when a three-point flexural test is conducted.

The force-indentation relationship is also distorted by the loading eccentricity of the indenter. Figure 15 shows that the greater the off-center distance, the earlier the force-indentation curve deviates from that corresponding to zero loading eccentricity. For example, if an off-center distance of up to $(5/4)h$ exists, the curve separates from the rest curves at the very beginning. Note that the indentation value is always calculated from the cross section where the first contact point is located, i.e., point A is Fig. 1, which is where the measurement is usually done during a flexural test.

Conclusions

An analytical method using an exact Green's function derived from the anisotropic elasticity theory has been successfully developed to investigate the contact behavior between composite laminates and rigid cylindrical indenters. The response of a laminate can be characterized into small and large contact stages as a result of curvature conformation of the laminate to the indenter in the contact region. In transition from the small to the large contact stages, the contact pressure distribution changes from an elliptical to a saddle shape with the contact length increasing progressively and rebounding of the $F-\alpha$ curve. The stress concentration in the laminate also decreases gradually. Use of large indenters or laminates with large span-to-thickness ratios allows a laminate to advance into the large contact stage early, and thus a higher tested strength of the laminate in a flexural test may be obtained. It is also found that change of the laminate thickness affects the $F-\alpha$ relationship more significantly than change of the laminate span does. In addition, it is always important to align the indenter at the correct position to avoid distortion of the $F-\alpha$ relationship and the asymmetric contact pressure distribution. Furthermore, changing the stacking sequence of a laminate has a negligible effect on the force-indentation relationship in the small contact stage.

Acknowledgment

This work was supported by the National Science Council of the Republic of China under Contract NSC-79-0401-E-002-33.

References

[1]Berg, C. A., Tirosh, J., and Israeli, M., "Analysis of Short Beam Bending of Fiber Reinforced Composites," *Composite Materials: Testing and Design (Second Conference),* American Society for Testing and Materials, ASTM STP 497, 1972, pp. 206–218.

[2]Tarnopol'skii, Y. M., Zhigun, I. G., and Polyakov, V. A., "Distribution of Shearing Stresses Under Three-Point Flexure in Beams Made of Composite Materials," *Polymer Mechanics,* Vol. 13, No. 1, 1977, pp. 52–58.

[3]Sandorff, P. E., "Saint-Venant Effects in an Orthotropic Beam," *Journal of Composite Materials,* Vol. 14, July 1980, pp. 199–212.

[4]Whitney, J. M., "Elasticity Analysis of Orthotropic Beams under Concentrated Loads," *Composites Science and Technology,* Vol. 22, 1985, pp. 167–184.

[5]Keer, L. M., and Miller, G. R., "Smooth Indentation of Finite Layer," *Journal of Engineering Mechanics,* Vol. 109, No. 3, 1983, pp. 706–717.

[6]Sankar, B. V., and Sun, C. T., "Indentation of a Beam by a Rigid Cylinder," *International Journal of Solids and Structures,* Vol. 19, No. 4, 1983, pp. 293–303.

[7]Keer, L. M., and Ballarini, R., "Smooth Contact Between a Rigid Indenter and an Initially Stressed Orthotropic Beam," *AIAA Journal,* Vol. 21, No. 7, 1983, pp. 1035–1045.

[8]Sun, C. T., and Sankar, B. V., "Smooth Indentation of an Initially Stressed Orthotropic Beam," *International Journal of Solids and Structures,* Vol. 21, No. 2, 1985, pp. 161–176.

[9]Sankar, B. V., "Smooth Indentation of Orthotropic Beams," *Composites Science and Technology,* Vol. 34, 1989, pp. 95–111.

[10]Sankar, B. V., "An Integral Equation for the Problem of Smooth Indentation of Orthotropic Beams," *International Journal of Solids and Structures,* Vol. 25, No. 3, 1989, pp. 327–337.

[11]Pagano, N. J., "Exact Solutions for Composite Laminates in Cylindrical Bending," *Journal of Composite Materials,* Vol. 3, 1969, pp. 398–411.

[12]Wu, E., and Yen, C.-S., "The Contact Behavior Between Laminated Composite Plates and Rigid Spheres," *Journal of Applied Mechanics* (to be published).

[13]Choi, H. Y., Wu, H.-Y., and Chang, F.-K., "A New Approach toward Understanding Damage Mechanisms and Mechanics of Laminated Composites Due to Low-Velocity Impact: Part II—Analysis," *Journal of Composite Materials,* Vol. 25, Aug. 1991, pp. 1012–1038.

[14]Chao, J.-C., "A Study for Contact of Laminated Composites," M.S. Thesis, National Taiwan Univ., Taipei, Taiwan, ROC, 1991.